Tripathi et al., https://doi.org/10.1083/jcb.201703105

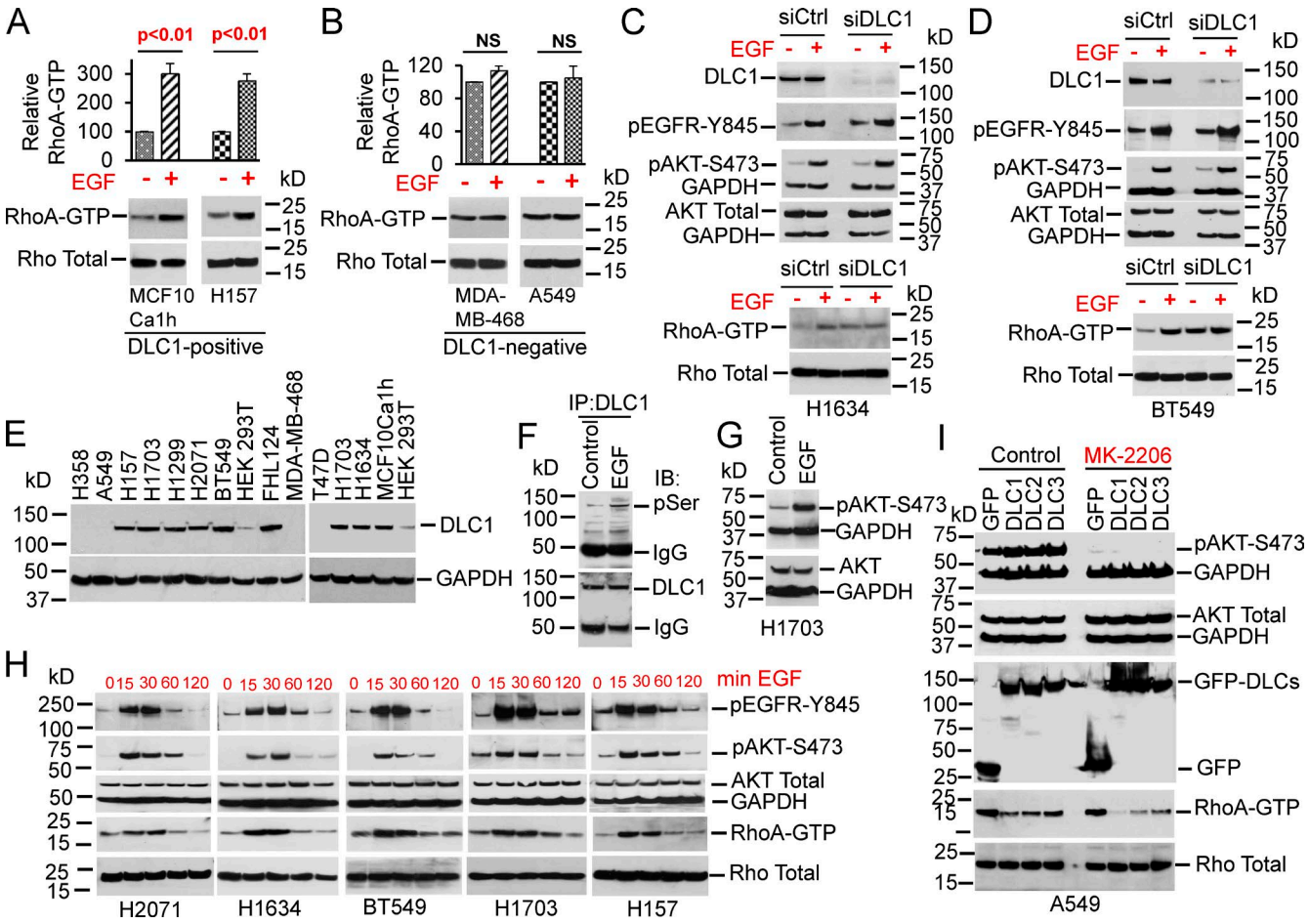

Figure S1. **EGF-induced AKT activity increases RhoA-GTP through DLC1; AKT regulates all three DLC genes.** (A) EGF increased RhoA-GTP, but not total Rho, in the MCF10Ca1h breast cancer cell line and H157 in the NSCLC line; both of which express DLC1. The graph shows the relative RhoA-GTP means ± SD from three experiments. Parametric two-tailed *t* tests were performed for statistical analysis. (B) Experimental conditions were similar for MDA-MB-468 breast cancer cell line and A549 NSCLC cell line, which were DLC1 negative. EGF did not alter RhoA-GTP in the DLC1-negative lines. Error bars in the graph indicate the SD. (C and D) siRNA knockdown of DLC1 in H1634 and BT549 cells resulted in RhoA-GTP being unresponsive to EGF. Knockdown of DLC1 expression by siRNAs (top) in H1634 (C) and BT549 (D) cells. EGF-stimulated EGFR phosphorylation and AKT activity in both DLC1-expressed and DLC1-knocked-down cells. However, EGF did not alter the total AKT or GAPDH, whether DLC1 was expressed or knocked down. Knockdown of DLC1 abrogated the ability of EGF to increase RhoA-GTP. EGF stimulates RhoA-GTP only in DLC1-positive cells (compare lanes 1 and 2 in the RhoA-GTP blot), but not in DLC1-knocked down cells (compare lanes 3 and 4 in the RhoA-GTP blot) for H1634 (C) and BT549 (D). EGF did not alter total Rho whether DLC1 was expressed or knocked down (bottom). (E) Relative expression of DLC1 protein (top) in the indicated cell lines. GAPDH was used as a loading control. (F) EGF increased the phosphorylation of AKT serines in DLC1 (pSer) without changing total DLC1. Lysates from H1703 cells treated with or without EGF were IP with DLC1 antibody, followed by IB with phospho-AKT substrate-specific (top) or DLC1 (bottom) antibodies. (G) EGF substantially increased AKT activity, as measured by pAKT-S473 (top), without changing the AKT level (bottom). GAPDH was used as a loading control. (H) Time course of EGF-induced responses to EGFR activity, AKT activity, and RhoA-GTP. There is good correlation between increased EGFR activity (top; measured by EGFR phosphorylation at tyrosine 845), increased AKT activity (as measured by phosphorylation of AKT-serine 473 [pAKT-S473]), and increased RhoA-GTP activity in all DLC1-positive lines by EGF treatment. EGF did not alter the total AKT (middle) and the total Rho (bottom). GAPDH was used as a loading control. (I) A549 cells, transfected with GFP, DLC1, DLC2, or DLC3 constructs, were treated without or with AKT inhibitor MK-2206. Compared with GFP vector, transfection of DLC1, DLC2, or DLC3 decreased RhoA-GTP (control), but not total Rho (control). MK-2206 reduced AKT activity (pAKT-S473) but not total AKT or total Rho. The effect of MK-2206 on RhoA-GTP in DLC2- and DLC3-transfected cells was less than its effect on DLC1-transfected cells (MK-2206; GFP-DLCs). Expression of GFP, DLC1, DLC2, and DLC3 in the presence or absence of MK-2206 (middle).

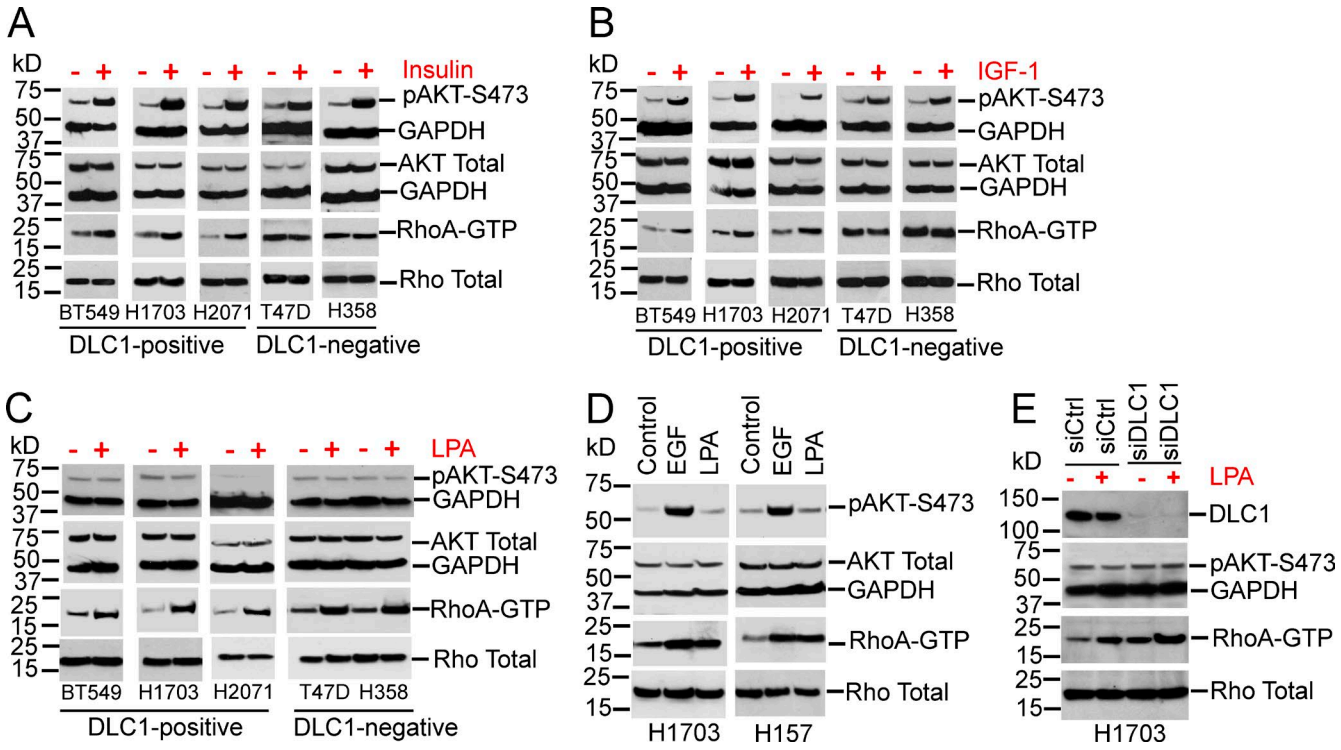

Figure S2. **Insulin and IGF-1 induce AKT activity and increase RhoA-GTP through DLC1; LPA induces RhoA-GTP in a DLC1-independent manner and does not activate AKT.** (A) Insulin increased RhoA-GTP (lower middle) in DLC1-positive BT549, H1703, and 2071 cell lines but not in DLC1-negative T47D or H358 lines, although insulin treatment increased AKT activity in all lines (top). Insulin did not alter the total AKT (upper middle) and the total Rho (bottom). GAPDH was used as a loading control. (B) Experimental conditions and data display are as in A, except cells were treated with IGF-1. IGF-1 increased RhoA-GTP in DLC1-positive BT549, H1703, and 2071 lines but did not alter RhoA-GTP in DLC1-negative T47D or H358 lines (lower middle), although IGF-1 treatment increased AKT activity in all lines (top). (C) LPA increased RhoA-GTP in both DLC1-positive and DLC1-negtive lines (bottom middle). However, LPA treatment did not alter AKT activity (top), total AKT (top middle), or total Rho level (bottom). (D) LPA treatment did not stimulate AKT activity (top), unlike EGF treatment, in H1703 and H157 lines. However, LPA increased RhoA-GTP comparable to EGF treatment (lower middle) in both lines. (E) LPA increased RhoA-GTP (bottom middle) in H1703 cells in which DLC1 expression has been knocked down by siRNAs (top). However, LPA did not alter AKT activity (top middle) and total Rho level (bottom). GAPDH was used as loading control.

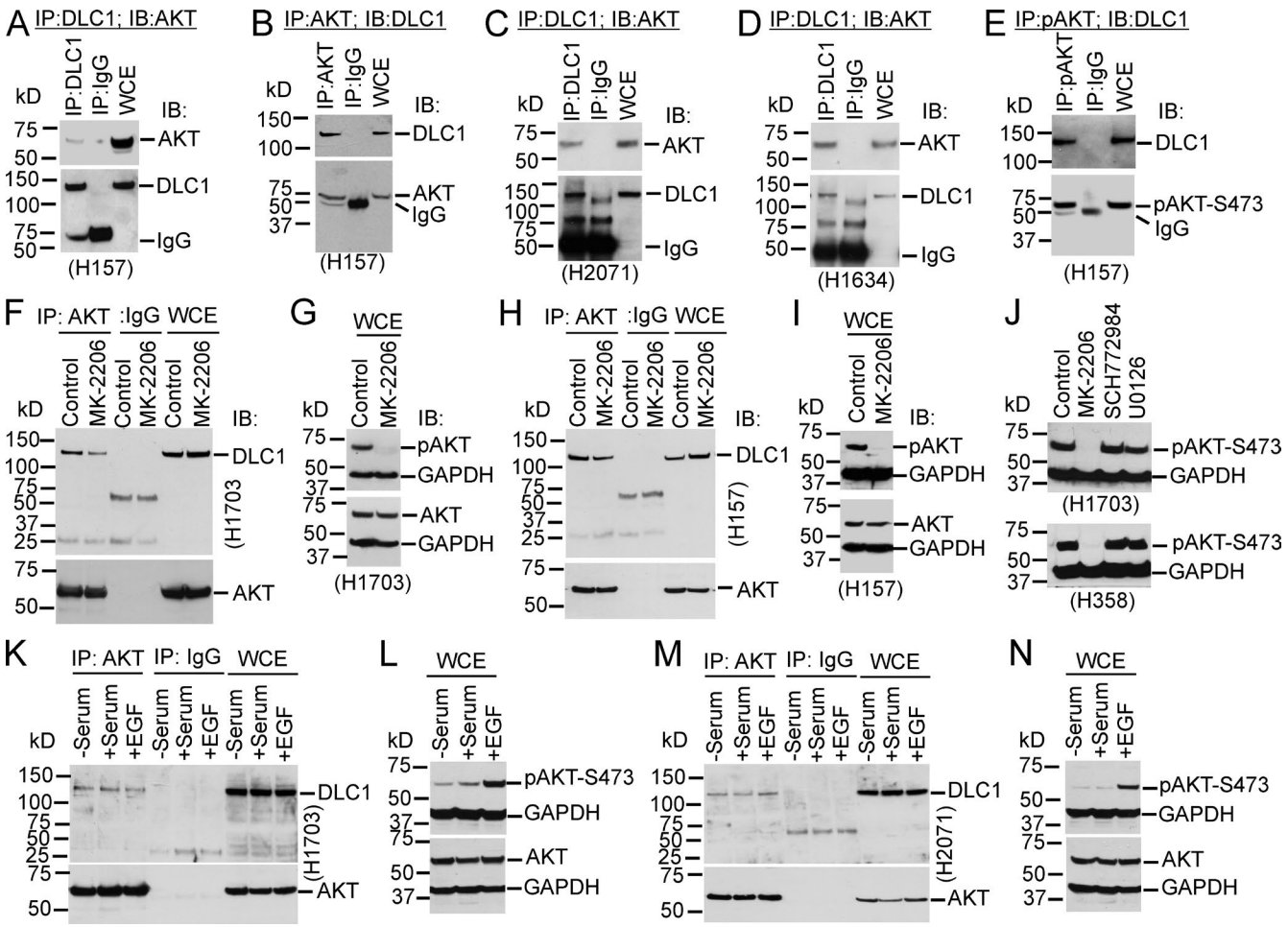

Figure S3. **DLC1 and AKT forms a protein complex in human cell lines, and complex formation does not require enzymatic activity of AKT.** (A) Endogenous protein complex between DLC1 and AKT. Lysates from H157 cells were IP with DLC1 or mock IgG antibodies followed by IB with AKT (top) or DLC1 (bottom) antibodies. WCE, whole cell extract. (B) The endogenous protein complex between DLC1 and AKT was confirmed by reciprocal coIP. (C and D) Experimental conditions and data display were similar to A, but for nontransformed lines H2017 (C) and H1634 (D). (E) Some AKTs that are associated with DLC1 are enzymatically active. Endogenous protein complex between DLC1 and kinase-active AKT (pAKT-S473) in H157 cells. Lysates were IP with pAKT-S473 antibody followed by IB with DLC1 (top) or pAKT-S473 (bottom) antibodies. (F) Complex formation between DLC1 and AKT did not require AKT enzymatic activity. The experimental conditions were similar to B, except that the protein complex between DLC1 and AKT was analyzed in the absence or presence of MK-2206 in H1703 cells. (G) MK-2206 treatment inhibited AKT activity (measured by pAKT-S473) in H1703 cells. (H) The experimental conditions and data display were similar to F, but for H157 cells. (I) MK-2206 treatment inhibited AKT activity in H157 cells. (J) MK-2206 is a specific AKT inhibitor because AKT activity (measured by pAKT-S473) was inhibited by MK-2206 in both H1703 and H358 lines but not by inhibitors of ERK (SCH772984) or MEK (U0126). (K–N) Stimulation of AKT by EGF treatment did not increase the AKT/DLC1 protein complex in H1703 (K) and H2071 (M) cell lines. EGF stimulated AKT activity, but not total AKT, in H1703 (L) and H2071 (N) lines. GAPDH was used as a loading control.

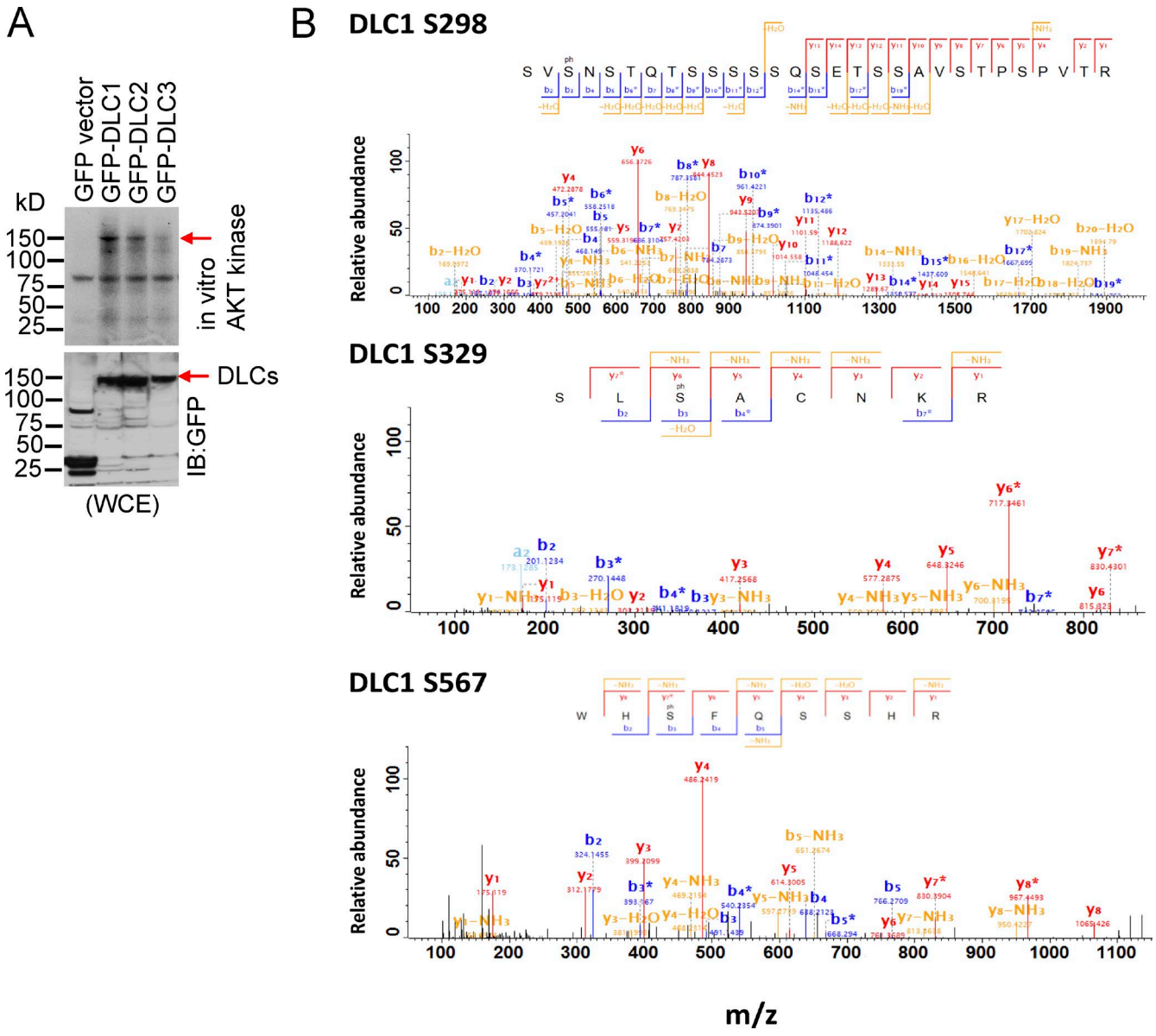

Figure S4. **DLC1, DLC2, and DLC3 are AKT substrates.** (A) In vitro AKT kinase assay. (A, top) IP DLC1-WT was strongly phosphorylated by recombinant AKT kinase (lane 2), as detected with ^{32}P autoradiography. GFP control gave no phosphorylation signal (lane 1). DLC2 (lane 3) and DLC3 (lane 4) were also phosphorylated, but weakly compared with DLC1. (A, bottom) Expression of GFP vector and GFP-tagged DLC constructs. (B) DLC1 phosphopeptides identified by mass spectrometry. Annotated tandem mass spectrometry spectra are shown for the three phosphopeptides containing phosphorylated S298, S329, and S567. b-Type fragments are shown in blue and y-type fragments in red. Water- and ammonia-loss peaks are shown in yellow, and neutral phosphate losses are indicated with asterisks. The fragment ions observed allow full localization of the phosphorylation sites on the serine residues noted in each peptide. Spectra were annotated using the Viewer software of the MaxQuant 1.3.0.5 software package.

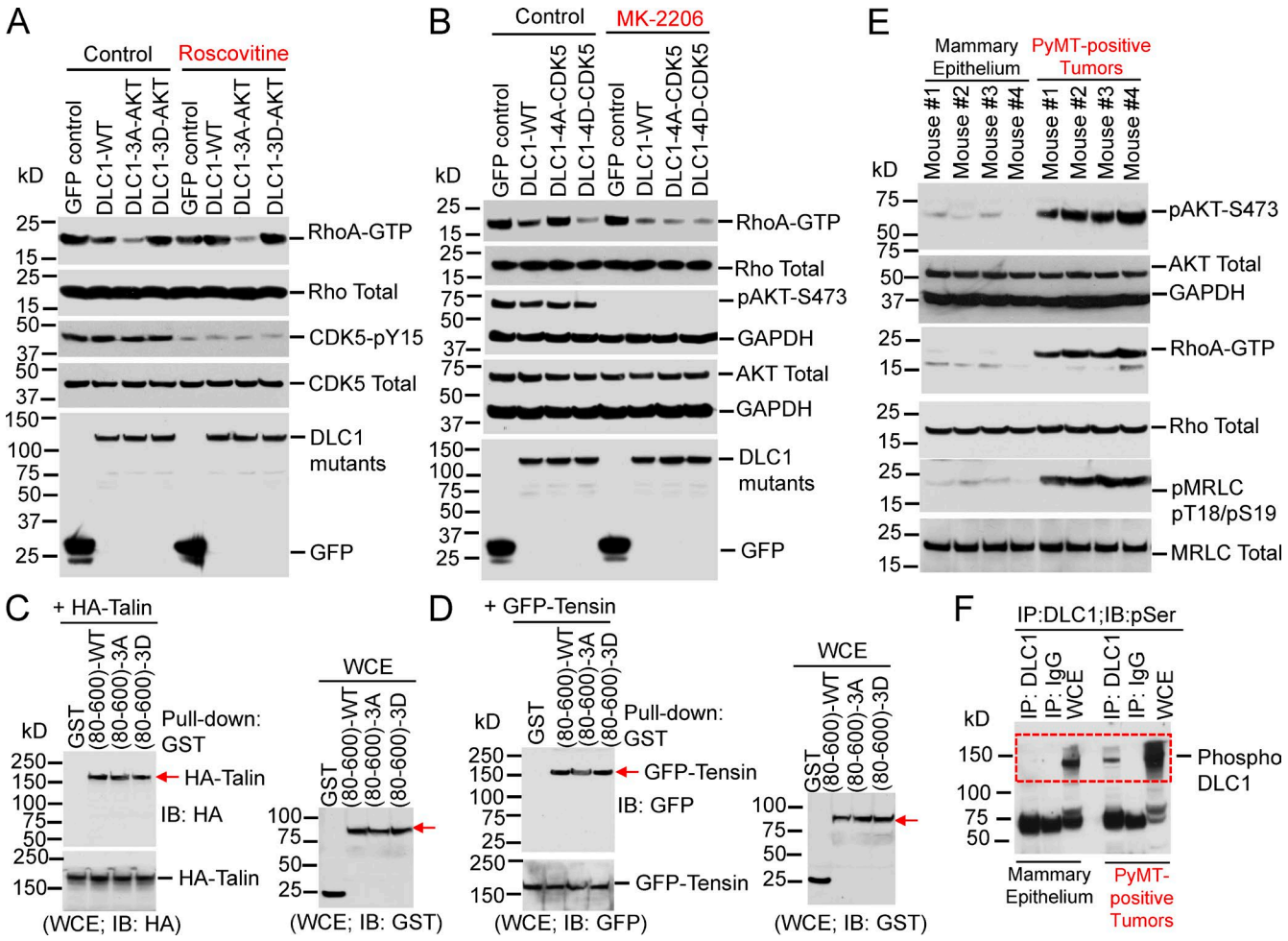

Figure S5. **AKT phosphorylation of DLC1 is phenotypically dominant over CDK5 phosphorylation of DLC1; MMTV-PyMT–positive tumors have high AKT activity, high RhoA-GTP, and high phosphorylation of DLC1 serines.** (A) Effect of CDK5 inhibitor roscovitine on RhoGAP activity of DLC1 mutants for AKT sites. RhoA-GTP (top) and total Rho (middle) in A549 cells expressing the indicated DLC1 mutants (bottom). RhoA-GTP was reduced by DLC1-WT or DLC1-3A mutant compared with GFP control and DLC1-3D mutant (control). Roscovitine induced an increase in RhoA-GTP in DLC1-WT (compare lanes 2 and 6) but did not influence RhoA-GTP in GFP, DLC1-3A, or DLC1-3D mutant for AKT sites (roscovitine), although roscovitine efficiently suppressed the CDK5 kinase activity, as measured by CDK5-pY15, in each transfectant (middle). Roscovitine did not affect the CDK5 level. (A, bottom) Expression of each transfectant. (B) Effect of MK-2206 on RhoGAP activity of DLC1 mutant for CDK5 sites. RhoA-GTP (top) and total Rho (middle) in A549 cells expressing the indicated DLC1 mutants (bottom). RhoA-GTP was reduced by DLC1-WT and DLC1-4D mutant (for CDK5 sites) compared with GFP control and DLC1-4A mutant (control). MK-2206 reduced RhoA-GTP in DLC1-WT, as well as in 4A and 4D mutants of the CDK5 sites, but not in GFP control (MK-2206). MK-2206 efficiently suppressed the AKT activity, as measured by pAKT-S473, in each transfectants (middle), but not total AKT. (B, bottom) Expression of each transfectant. (C and D) The decreased binding of tensin and talin protein to DLC1-3D was not an intrinsic property of the transfected linker region by itself. Immunoblots from HEK 293T cells cotransfected with HA-tagged full-length talin (C) or GFP-tagged full-length tensin (D) and GST, GST-DLC1 (80–600)-WT, GST-DLC1 (80–600)-3A, or GST-DLC1 (80–600)-3D fragment was pulled down with GST antibody and IB with HA antibody (C) or GFP antibody (D; top). IB with HA or GFP (bottom) antibodies to show expression of HA or GFP-tagged construct. IB with GST antibodies (C and D, right) to show the expression of GST-tagged DLC1 constructs. The GST-DLC1 (80–600)-3D bound talin and tensin as efficiently as GST-DLC1 (80–600)-WT. Each immunoblot is representative of at least two independent experiments. (E) Tumors from MMTV-PyMT-positive mice have high AKT activity (measured by pAKT-S473; top, lanes 5–8), high RhoA-GTP (middle, lanes 5–8), and high RhoA-ROCK-dependent pMRLC (lanes 5–8) compared with mammary epithelium from pregnant mice (compare with lanes 1–4 in the respective blot). However, total AKT, total Rho, and total MRLC levels from each tissue were similar. GAPDH was used as a loading control. (F) Lysates from mammary epithelium of pregnant mice or MMTV PyMT-positive tumors were IP with DLC1 antibody followed by IB with phospho-AKT substrate-specific (pSer) antibody. WCE, whole cell extract. IP DLC1 from MMTV PyMT-positive tumors was strongly phosphorylated compared with IP DLC1 from mammary epithelium of pregnant mice.

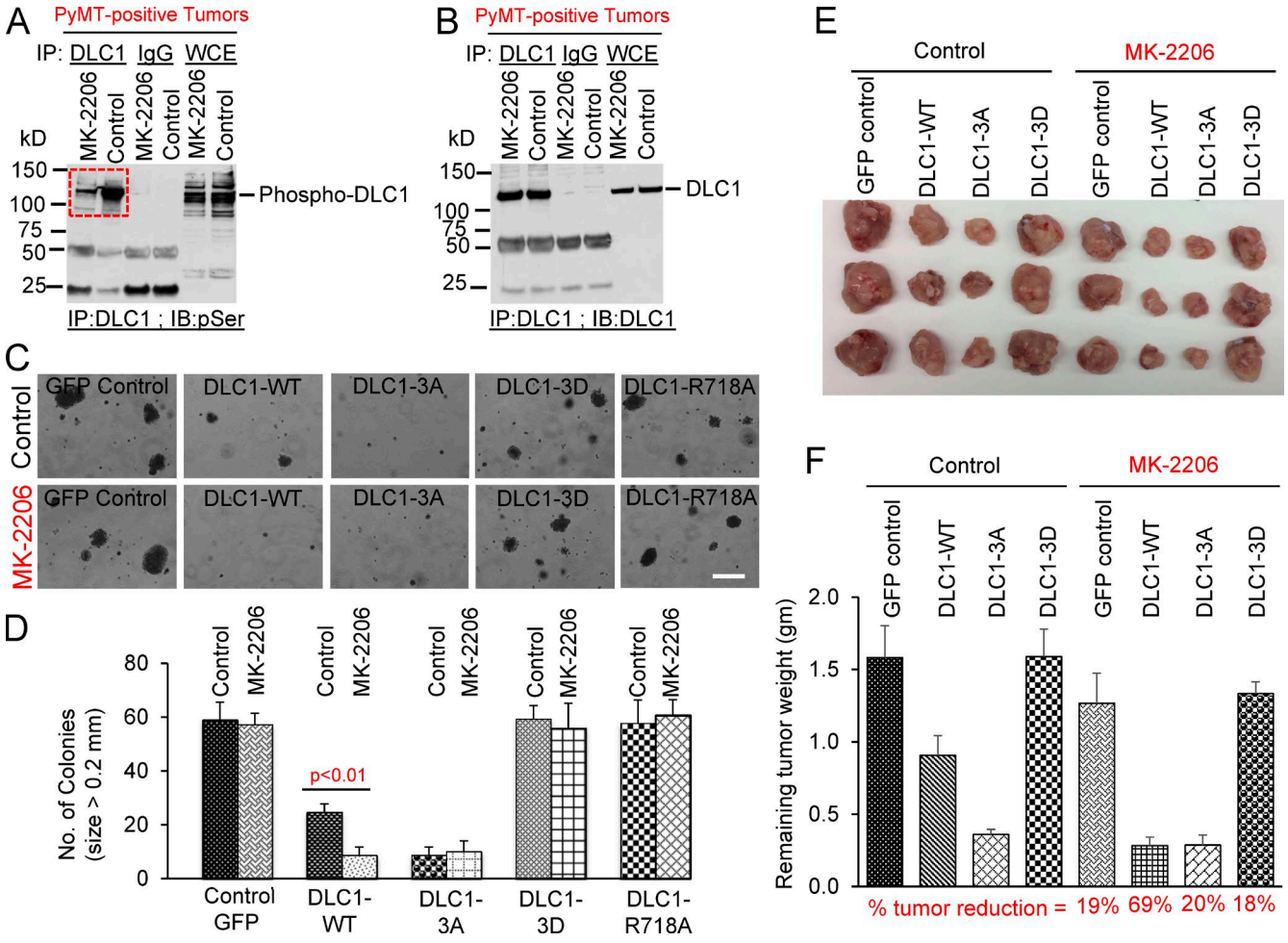

Figure S6. **AKT inhibition has greater antitumor activity in DLC1-positive tumors.** (A and B) Lysates from MMTV PyMT–positive tumors treated with or without MK-2206 were IP with DLC1 antibody followed by IB with (pSer) phospho-AKT substrate-specific (A) or DLC1 (B) antibodies. WCE, whole cell extract. MK-2206 treatment reduced serine phosphorylation (pSer) of DLC1 (A; compare lanes 1 and 2) without changing the DLC1 expression (B; compare lanes 1 and 2). (C) Anchorage-independent growth of H358 cells stably transfected with DLC1 mutant in the absence or in the presence of MK-2206. MK-2206 treatment inhibited growth and colony formation in soft agar of DLC1-WT transfected cells. However, MK-2206 treatment did not influence the anchorage-independent growth or the number of soft agar colonies of GFP control, DLC1-3A, DLC1-3D, or GAP-dead DLC1-R718A transfected cells. Bar, 2 mm. (D) Quantification of agar colonies (>0.4 mm) in the indicated groups from three independent experiments. Parametric two-tailed *t* tests were performed for statistical analysis. MK-2206 treatment induced a significant decrease ($P < 0.01$) in soft agar colonies in DLC1-WT. However, MK-2206 treatment did not influence the soft agar growth of GFP, DLC1-3A, DLC1-3D, or DLC1-R718A transfected cells. Error bars in the graph indicate the SD. (E) Mice with tumors were treated with MK-2206 (50 mg/kg for 5 d) 8 wk after injecting the stable transfectants. Photographs of xenograft tumors from mice after treatment for 5 d with MK-2206. (F) Graph shows tumor weight (in grams) means ± SD for each group in the presence or absence of MK-2206 treatment. The numbers below the graph represent the percent reduction in tumor weight by MK-2206 treatment compared with respective untreated group.

Table S1. **Primers used for engineering DLC1 plasmids**

Primer name	Sequence (5′–3′)
DLC1-S298A-Forward	GAGGAGCGTTGCCAACTCCACGCAGACC
DLC1-S298A-Reverse	GGTCTGCGTGGAGTTGGCAACGCTCCTC
DLC1-S298D-Forward	GAGGAGCGTTGATAACTCCACGCAGACC
DLC1-S298D-Reverse	GGTCTGCGTGGAGTTATCAACGCTCCTC
DLC1-S329A-Forward	CCCGGAGCCTCGCTGCGTGCAACAAGC
DLC1-S329A-Reverse	GCTTGTTGCACGCAGCGAGGCTCCGGG
DLC1-S329D-Forward	CCCGGAGCCTCGATGCGTGCAACAAGC
DLC1-S329D-Reverse	GCTTGTTGCACGCATCGAGGCTCCGGG
DLC1S567A-Forward	CTGAGATGGCACGCTTTCCAGAGCTCA
DLC1S567A-Reverse	TGAGCTCTGGAAAGCGTGCCATCTCAG
DLC1S567D-Forward	CTGAGATGGCACGATTTCCAGAGCTCA
DLC1S567D-Reverse	TGAGCTCTGGAAATCGTGCCATCTCAG